

Observation of twin-beam-type quantum correlation in optical fiber

Jay E. Sharping, Marco Fiorentino, and Prem Kumar

Center for Photonic Communications and Computing, Department of Electrical Engineering, Northwestern University, 2145 North Sheridan Road, Evanston, Illinois 60208-3118

Received September 18, 2000

We report generation of pulsed twin beams of light through optical parametric amplification in a fiber Sagnac loop. By pumping the Sagnac loop with picosecond pulses at a wavelength near the zero-dispersion wavelength of the fiber, we achieve phase-matched nondegenerate four-wave mixing with gain. For a gain of 2.2, the intensity noises of the amplified signal and the generated idler (conjugate) pulses are found to be correlated by 5.0 dB, and the subtracted noise drops below the shot-noise limit by 1.1 dB (2.6 dB when corrected for losses). We have investigated the gain dependence of the quantum-noise reduction as well as of the intensity noises of the amplified signal and idler pulses. As the gain increases, we observe the onset of excess noise on the idler pulses. © 2001 Optical Society of America

OCIS codes: 060.2320, 060.4370, 190.4380, 190.4970, 270.6570.

Parametric downconversion in $\chi^{(2)}$ materials has been the primary mechanism for the generation of polarization-entangled photon-pair pulses that were used in recent teleportation experiments.^{1,2} A formidable engineering problem lies in the demonstration, transmission, storage, and use of quantum entanglement over long distances.³ The desire for long-distance propagation and the need to minimize optical losses to preserve the entanglement suggest that standard optical fiber should be used in its 1.5- μm low-loss transmission window. A fiber-based scheme for the generation of entangled photon pairs is thus desirable and would have an obvious advantage over other approaches because it is directly compatible with the propagation medium.

One step toward demonstrating a fiber-based scheme for the generation of entangled photon pairs is creating correlated photons through nondegenerate four-wave mixing (FWM) in the fiber. Two photons of a strong pump at angular frequency ω_p are coupled via the $\chi^{(3)}$ nonlinearity of the fiber to create signal and idler (conjugate) photons at frequencies $\omega_s = \omega_p - \Omega$ and $\omega_i = \omega_p + \Omega$, respectively. Since each generated signal photon is accompanied by a generated idler photon, the two form correlated "twin" beams. Entanglement follows from creative manipulation and combination of such correlated photon pairs. At visible frequencies, polarization modulation instability in optical fibers has been demonstrated where a variable birefringence was used to adjust the gain profile.⁴ Recently, our group demonstrated a widely tunable fiber-optic parametric oscillator that is based on the FWM gain and emits picosecond pulses that are tunable over 70 nm near the pump wavelength near 1.5 μm .⁵ To demonstrate the generation of twin beams, one needs to detect and measure the quantum correlation between the amplified signal and the idler pulses generated in a single pass through such a device.⁶ In this Letter we report what we believe to be the first observation of twin-beam-type quantum-noise correlation in a fiber-optic device.

A nonlinear fiber Sagnac interferometer (NFSI) provides a convenient means of separating the pump

from the amplified signal and idler produced in the FWM process, while still allowing mixing among them.⁷ The NFSI consists of a 50/50 standard fused-silica coupler with two ports spliced to opposite ends of a dispersion-shifted fiber (DSF) to create a loop. A fiber polarization controller placed within the loop provides a phase bias between the counter-propagating waves, allowing the device to be operated as a total reflector. FWM within the loop is phase matched⁸ by use of a strong pump near the zero-dispersion wavelength (λ_0) of the DSF. In our experiment a small signal is injected into the loop, so the device operates as a fiber-optic parametric amplifier.

The experimental setup is illustrated in Fig. 1. We create the pump and the input signal pulses by taking the 75-MHz train of 150-fs pulses centered at 1535 nm from a Ti:sapphire-pumped optical parametric oscillator system (Coherent, Inc., Models Mira 900 and Mira OPO), dispersing them with a grating and then spectrally filtering them to obtain two synchronous beams with a tunable wavelength separation of 5–15 nm. This arrangement gives 4.0-ps pump pulses of ≈ 10 -W peak power and 2.8-ps signal pulses of ≈ 3 -W peak power. The pump and signal beams obtained in this way are shot-noise limited to within the accuracy of our measurement setup (± 0.2 dB). The pump is injected directly into the left-hand arm of the Sagnac loop, and 10% of the signal, obtained with a 90/10 coupler, enters the right-hand arm (see

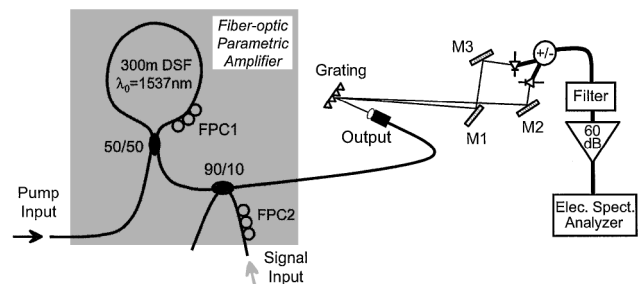


Fig. 1. Schematic of the experimental setup. M1–M3, mirrors. See text for other definitions.

Fig. 1). We adjust the optical paths traversed by the input pump and signal pulses to maximize the pulse overlap in the loop. The loop consists of 300 m of DSF with $\lambda_0 = 1537 \pm 2$ nm, for which we expect ~ 1 ps of temporal walk-off between the signal and pump. The intraloop fiber polarization controller (FPC1) is adjusted so that the loop behaves as a total reflector; < -30 dB of the pump's average power leaks into the signal arm of the NFSI. An additional fiber polarization controller (FPC2) is used to adjust the input signal polarization for efficient FWM in the loop. Counterpropagating idler pulses are generated in the loop, owing to FWM in the clockwise and counterclockwise directions. Their phases are such that the counterpropagating idler pulses, on arriving at the 50/50 coupler, interfere constructively on the right-hand port of the coupler and destructively on the left-hand port (cf. Fig. 1).⁷ Thus the idler emerges from the same port of the NFSI as the amplified input signal.

After passing through the 90/10 coupler, the generated idler and the amplified signal pulses are brought into free space and separated by use of a low-loss diffraction grating. The diffraction efficiency is maximized by use of wave plates (not shown in Fig. 1) to adjust the polarization of the signal and idler beams emerging from the fiber. The separated signal and idler beams are then focused onto two identical photodetectors. The overall optical loss for the amplified signal and idler pulses in the system is -3.1 dB (-0.85 dB in the Sagnac loop, -0.57 dB at the 90/10 coupler, -0.82 dB from the detection optics, and -0.82 -dB quantum efficiency of the detectors), corresponding to an overall detection efficiency of 49%.

The detectors are composed of photodiodes (Epitaxx Model ETX500T) that are mounted in a circuit that is resonant at 28 MHz. We first pass the photocurrent through a 50-MHz-cutoff low-pass filter to reject the 75-MHz mode beats of the source. A 12.5-MHz frequency range near 25 MHz is then selected with a bandpass filter, and the filtered photocurrent is amplified by 60 dB with a low-noise electronic amplifier, whose output is fed to a spectrum analyzer for making the noise measurements. The circuit allows monitoring of the average, i.e., dc, photocurrent as well as the sum- and difference-noise photocurrents at 28 MHz. During data acquisition a comparison is made between the difference-noise photocurrent of the beams under test and the shot-noise level, which is determined by direction of a portion of our shot-noise-limited pump onto the detectors such that the dc photocurrent produced at each detector matches that produced by the beams under test. The electronic noise floor of the instrumentation is also measured and subtracted from the data.

Noise generation during amplification was theoretically explored in detail by Caves.⁹ Aytür and Kumar⁶ applied the analysis to their experimental study of noise in optical parametric amplification, i.e., three-wave mixing, in $\chi^{(2)}$ materials. Similar analysis also holds for FWM in $\chi^{(3)}$ materials in the undepleted pump approximation. Including the effect

of subunity detection efficiency, one arrives at the following expression for quantum-noise reduction:

$$R = \langle \Delta \hat{I}^2 \rangle / \langle \Delta \hat{I}_C^2 \rangle = 1 - \eta + \eta / (2g - 1), \quad (1)$$

where η is the overall detection efficiency and g is the FWM gain. Here, quantum-noise reduction is defined as the ratio of the observed noise density of the difference photocurrent, $\langle \Delta \hat{I}^2 \rangle$, to the noise density of the difference photocurrent, $\langle \Delta \hat{I}_C^2 \rangle$, when coherent states of the same average photon number are incident upon the signal and idler detectors. The noise contributed to the signal and idler beams by the FWM gain is given by

$$\langle \Delta \hat{I}_{S(I)}^2 \rangle / \langle \Delta \hat{I}_{S(I),C}^2 \rangle = 2\eta(g - 1) + 1, \quad (2)$$

where $\langle \Delta \hat{I}_{S(I)}^2 \rangle$ is the observed noise-power density of the photocurrent generated by the amplified signal (idler) and $\langle \Delta \hat{I}_{S(I),C}^2 \rangle$ is that for a coherent state of the same average photon number.

A typical plot of the observed noise reduction versus FWM gain is shown in Fig. 2. The inset shows optical spectra of the pump and the signal and idler pulses before and after amplification. In Fig. 3 we show plots of the noise above the shot-noise level for the amplified signal and idler beams as a function of the FWM gain. The error bars in both figures represent the standard error based on the variances of our measured data.

The data in Fig. 2 show that there is a quantum-noise correlation between the amplified signal beam and the idler beam generated in our fiber-optic parametric amplifier. The maximum noise correlation is 5.0 dB at a gain of 2.2, since the difference noise at this gain falls below the sum noise by 5.0 dB. In addition, the difference noise falls below the shot-noise level by 1.1 dB (2.6 dB when corrected for losses), giving an observed quantum-noise reduction of $R = 0.8$. At low FWM gains, the data follows the trend expected from Eq. (1) for quantum-noise reduction R . As the gain increases beyond 2.5, the onset of some uncorrelated excess noise destroys the noise reduction.

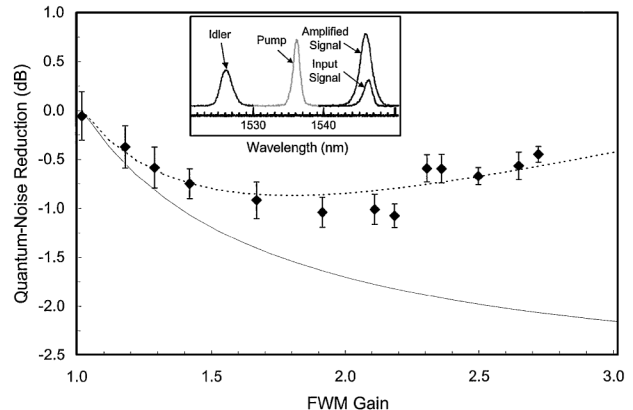


Fig. 2. Measured quantum-noise reduction as a function of the FWM gain, along with the predicted curve based on Eq. (1) for $\eta = 0.49$ (solid curve). The dashed curve represents a fit of the data to Eq. (3) with $A = 0.15$. The inset shows a typical FWM optical spectrum.

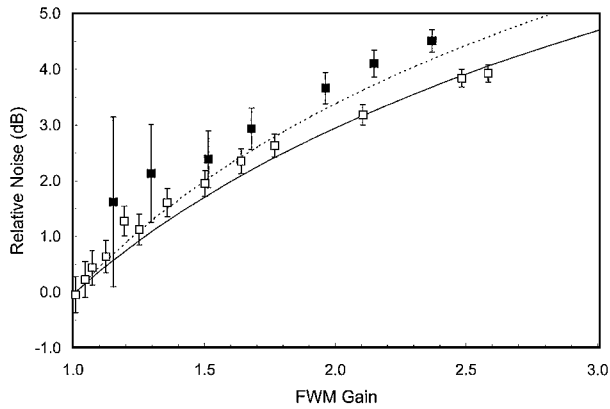


Fig. 3. Measured noise above shot noise as a function of the FWM gain for the amplified signal (open squares) and the idler (filled squares) pulses. The solid curve is a plot of Eq. (2) for $\eta = 0.49$, and the dashed curve is a plot including the excess noise.

The data agree reasonably well with a model that includes an arbitrary mechanism of linear excess noise according to

$$R' = \langle \Delta \hat{I}^2 \rangle / \langle \Delta \hat{I}_C^2 \rangle = 1 - \eta + \eta / (2g - 1) + A(g - 1), \quad (3)$$

which is shown by the dashed curve in Fig. 2. Here A determines the excess-noise contribution and $\eta = 0.49$ as measured in the experiment. Similarly, the dashed curve in Fig. 3 is a plot of Eq. (2) with this additional noise term for the same value of A . The physical origin of this excess noise is yet unclear, but we have observed the following: The choice of the pump wavelength, λ_p , is critical to achieving the noise reduction. We were unable to observe sub-shot-noise behavior for λ_p even slightly longer than λ_0 of the DSF. The best results were obtained for λ_p equal to or slightly shorter than λ_0 . The wavelength difference between the injected signal and the pump had little effect on the noise reduction, provided that there was measurable FWM gain for the chosen wavelengths.

Ideally, a parametric amplifier should add the same amount of noise to the signal and idler beams, but the data in Fig. 3 show that the idler-noise power is larger than the signal-noise power by as much as 1 dB and that the difference increases with FWM gain. This difference suggests that there is either larger loss in the signal beam or some additional mechanism that contributes noise to the idler. We have carefully measured the λ -dependent losses in our setup and found 5% greater loss in the idler beam than in the signal beam. Therefore we conclude that there must be some other mechanism that adds noise to the idler.

We have considered a number of potential physical mechanisms that add noise. Our setup can be adjusted so that other, undesirable, higher-order mixing processes occur among the idler, the pump, and the signal pulses. Such mixing does result in additional intensity noise, but in our measurements higher-order mixing was minimized to the extent that the power at the generated additional wavelengths was less than 1% of the amplified signal power. Guided acous-

tic-wave Brillouin scattering (GAWBS),¹⁰ which adds phase noise to the various pulses, also plays a role. In theory, direct detection as used in our experiment is insensitive to phase noise, so GAWBS should not be a factor. In practice, however, the detection scheme is sensitive to polarization noise, so cross-polarized GAWBS can result in intensity noise. By carefully adjusting the polarization state of the idler and the signal pulses and passing them through a low-loss polarizer before detection, we were able to filter out the cross-polarized GAWBS noise from our measurements. Copolarized GAWBS may still be present, but it does not contribute to the noise-reduction measurements. Raman scattering must also be considered.¹¹ The associated frequency shifts are very small for pulses of 1-nm spectral width spaced 5–15 nm apart. Measurements of Raman amplification of the signal pulses by the pump pulses in our experiment indicate a Raman gain of less than 5%. Self-phase modulation of the signal or the idler and cross-phase modulation between the pump and the signal or the idler would be a concern if the effect were large enough to cause spectral and temporal pulse-shaping effects. Typical spectra indicate that large amounts of self-phase and cross-phase modulation are not present on the signal and idler pulses. Self-phase modulation of the pump is certainly present, because a small amount is essential for achieving phase matching in the FWM process.

In conclusion, we have demonstrated twin-beam-type quantum correlation between the signal and idler pulses in a fiber-optic parametric amplifier. Although there seems to be an as-yet unidentified mechanism of excess noise on the idler, the correlation seems strong enough for further development of an all-fiber source of polarization-entangled photon pairs.

This research was supported in part by the U.S. Army Research Office under a collaborative grant from the Multidisciplinary University Research Initiative (MURI) program. J. Sharping's e-mail address is j-sharping@northwestern.edu.

References

1. D. Bouwmeester, J. W. Pan, K. Mattle, M. Eibl, H. Weinfurter, and A. Z. Zeilinger, *Nature* **390**, 575 (1997).
2. D. Boschi, S. Branca, F. De Martini, L. Hardy, and S. Popescu, *Phys. Rev. Lett.* **80**, 1121 (1998).
3. W. Tittel, J. Brendel, H. Zbinden, and N. Gisin, *Phys. Rev. Lett.* **81**, 3563 (1998).
4. S. G. Murdoch, R. Leonhardt, and J. D. Harvey, *Opt. Lett.* **20**, 866 (1995).
5. D. K. Serkland and P. Kumar, *Opt. Lett.* **24**, 92 (1999).
6. O. Aytür and P. Kumar, *Phys. Rev. Lett.* **65**, 1551 (1990).
7. K. Mori, T. Mirioka, and M. Saruwatari, *Opt. Lett.* **20**, 1424 (1995).
8. R. H. Stolen and J. E. Bjorkholm, *IEEE J. Quantum Electron.* **18**, 1062 (1982).
9. C. M. Caves, *Phys. Rev. D* **26**, 1817 (1982).
10. K. Bergman, H. A. Haus, E. P. Ippen, and M. Shirasaki, *Opt. Lett.* **19**, 290 (1996).
11. R. H. Stolen, E. P. Ippen, and A. R. Tynes, *Appl. Phys. Lett.* **20**, 62 (1972).